Journal of Medicinal Chemistry

Article

pubs.acs.org/jmc

Discovery of Novel, Potent, and Selective Inhibitors of 3-Phosphoinositide-Dependent Kinase (PDK1)

Sean T. Murphy,*[,†] Gordon Alton,[†] Simon Bailey,[†] Sangita M. Baxi,[†] Benjamin J. Burke,[†] Thomas A. Chappie,[‡] Jacques Ermolieff,[†] RoseAnn Ferre,[†] Samantha Greasley,[†] Michael Hickey,[†] John Humphrey,[‡] Natasha Kablaoui,[§] John Kath,[†] Steven Kazmirski,[§] Michelle Kraus,[†] Stan Kupchinsky,[†] John Li,[†] Laura Lingardo,[†] Matthew A. Marx,[†] Dan Richter,[†] Steven P. Tanis,[†] Khanh Tran,[†] William Vernier,[†] Zhi Xie,[†] Min-Jean Yin,[†] and Xiao-Hong Yu[†]

[†]Pfizer Global Research and Development, 10770 Science Center Drive, San Diego, California 92121, United States

[‡]Pfizer Global Research and Development, 558 Eastern Point Road, Groton, Connecticut 06340, United States

[§]Pfizer Global Research and Development, 620 Memorial Drive, Cambridge, Massachusetts 02139, United States

Supporting Information

ABSTRACT: Analogues substituted with various amines at the 6-position of the pyrazine ring on (4-amino-7-isopropyl-7H-pyrrolo[2,3-*d*]pyrimidin-5-yl)pyrazin-2-ylmethanone were discovered as potent and selective inhibitors of PDK1 with potential as anticancer agents. An early lead with 2-pyridine-3-ylethylamine as the pyrazine substituent showed moderate potency and selectivity. Structure-based drug design led to improved potency and selectivity against PI3Kα through a combination of cyclizing the ethylene spacer into a saturated, five-membered ring and substituting on the 4-position of the aryl ring with a fluorine. ADME properties were improved by lowering the lipophilicity with heteroatom replacements in the saturated, five-membered ring. The optimized analogues have a PDK1 K_i of 1 nM and >100-fold selectivity against PI3K/AKT-pathway kinases. The cellular potency of these analogues was assessed by the inhibition of AKT phosphorylation (T308) and by their antiproliferation activity against a number of tumor cell lines.

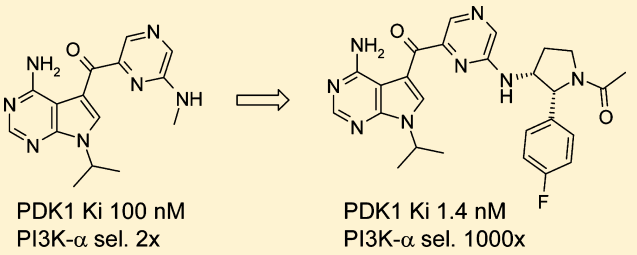

INTRODUCTION

3′-Phosphoinositide dependent kinase-1 (PDK1) belongs to the AGC family of kinases and was first identified by Kobayashi and Cohen.[1] PDK1 is part of the phosphoinositide-3 kinase (PI3K)/AKT pathway, which is one of the major cellular pathways involved in cell survival, differentiation, growth, and protein expression. This signal transduction pathway is downstream of several growth factor receptor tyrosine kinases (RTK's), such as the epidermal growth factor receptor, the insulin-like growth factor receptor-1, and the insulin receptor. Upon binding, these RTK's activate PI3Kα, which catalyzes the phosphorylation of phosphatidylinositol-(3,4)-biphosphate to generate biologically active phosphaditylinositol-(3,4,5)-triphosphate (PIP_3). The formation of PIP_3 triggers the colocalization at the membrane of two Ser/Thr kinases, PDK1 and AKT, both of which bind to PIP_3 through their pleckstrin homology (PH) domains. PDK1 phosphorylates the activation loop of AKT at threonine-308 (T308), thereby activating AKT to drive downstream signaling.[2]

PDK1 has been shown to be a critical regulator of the PI3K/AKT pathway, which is frequently activated in cancer cells due to either the loss of phosphatase and tensin homologue (PTEN) activity or the increase of PI3K/AKT activity.[3] A hypomorphic mutation of PDK1 protects PTEN± mice from developing a wide range of tumors.[4] Overexpression of PDK1 in murine mammary cells led to transformation, and isografts into syngenic mice led to tumor formation.[5] A recent review paper discusses evidence that PDK1 is implicated in human cancer and in resistance to chemotherapeutics.[6] As such, there is considerable activity in the pharmaceutical industry to develop potent PDK1 inhibitors.[7−10]

A number of PDK1 inhibitors have been reported in the literature, some of which are shown in Figure 1. The earliest examples (Figure 1**A**−**C**)[11−13] had been published at the time our work began. The work of Stauffer et al.[13] on the SAR of inhibitor **C** demonstrated that the cellular response when measuring AKT-T308 could be complicated by a lack of PI3K selectivity, and their cellular activity correlated better with PI3K inhibition than PDK1 inhibition. PI3K selectivity was not reported for the other early inhibitors (**A** and **B**), and we were concerned that they were not selective enough to test the antiproliferative effects of PDK1 inhibition. Furthermore, the report for inhibitor **B** showed a lack of correlation between PDK1 inhibition and cellular potency,[12] while inhibitor **A** is structurally similar to sunitinib, which is a potent inhibitor of many kinases.[14]

Received: July 30, 2011
Published: October 31, 2011

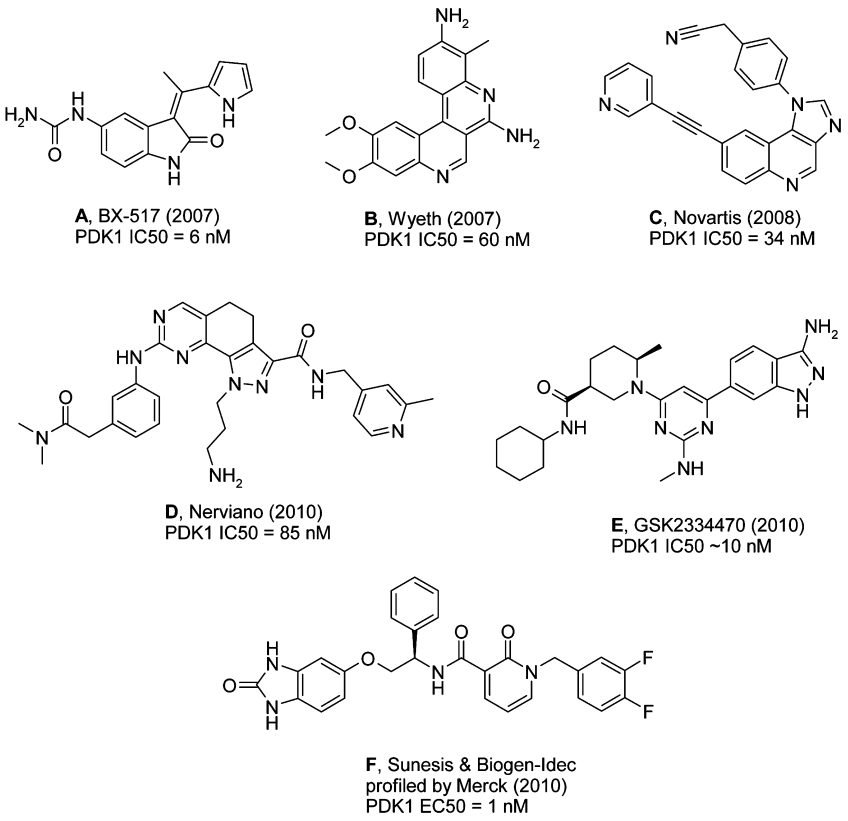

Figure 1. Selected PDK1 inhibitors disclosed in the literature.

More recently (while this manuscript was in preparation), three more papers have appeared describing potent and selective PDK1 inhibitors (Figure 1**D**–**F**).[8−10] Of particular note is compound **F**, described by co-workers at Sunesis and Biogen-Idec[15] and profiled by researchers at Merck.[10] It is equipotent with the optimized analogues described in this work and has excellent selectivity, and their biological results are consistent with our findings.

To enhance our confidence in the preclinical pharmacological assessment of PDK1 as an anticancer target, we sought potent PDK1 inhibitors with excellent selectivity over the other pathway kinases: PI3K, AKT, S6K, and mTOR. In the present study, we describe the discovery of 3-carbonyl-4-aminopyrrolopyrimidine analogues as potent PDK1 inhibitors with more than 100-fold selectivity against 38 of 39 kinases (97%), including the PI3K pathway kinases PI3K, AKT, S6K, and mTOR.

SYNTHESIS

The general synthesis for the analogues in this series is shown in Scheme 1. Reaction of chloropyrazine **1** (see Supporting Information for synthesis) with excess amine in a polar, aprotic solvent with cesium fluoride as a catalyst led to efficient displacement of the chloride. This reaction was broadly effective and provided access to several hundred analogues from a wide variety of primary and secondary amines.

Scheme 1. [a]

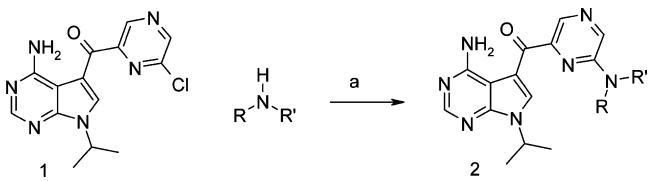

[a]Conditions: (a) diisopropylethylamine, cesium fluoride, anhydrous DMSO, 110−140 °C.

The *cis*-2-arylcyclopentylamines (**6a** and **6d**, X = CH_2) were synthesized by the method of Shepherd et al.[16] as shown in Scheme 2. The N-methyl analogue (**6e**) was synthesized by standard chemistry (see Scheme 2). The same general sequence was utilized to make the 3,4-disubstituted tetrahydrofuran (**6b**) and 3,4-disubstituted pyrrolidine (**6c**) analogues. After **6c** was coupled to **1**, the Boc group was removed with HCl in dichloromethane to give the final compound.

The synthesis of the 3,4-disubstituted tetrahydrofuran **7** (Scheme 3) followed the procedure of Andreotti and Ward.[17] The 3,4-disubstituted pyrrolidine analogues **13a**–**c** were made from aldehyde **8** using a phosphine-catalyzed [3 + 2] cycloaddition first disclosed by Lu and Xu.[18] The elimination of the sulfinate under basic conditions gave the pyrrole, which was then protected with the Boc group to give **10**. Reduction with Adams' catalyst gave the desired *cis*-stereochemistry on the pyrrolidine ring **11**. After saponification of the ester and Boc removal by treatment with acid, the amine was variously substituted with a Cbz, formyl, or acetyl group to give intermediates **12a**–**c**. The carboxylic acid was then converted into an amine via a Curtius rearrangement to give the desired amine products **13a**–**c**. Because a significant amount of des-Boc product was observed after the Curtius rearrangement, Boc anhydride was added to the reaction mixture to form the Boc-protected amine, which could then be easily purified by column chromatography.

After coupling intermediate **13a** to **1**, the Cbz group was removed by hydrogenolysis, which was followed by treatment with acetic anhydride to give the desired final product

dx.doi.org/10.1021/jm201019k | J. Med. Chem. 2011, 54, 8490−8500

Scheme 2. [a]

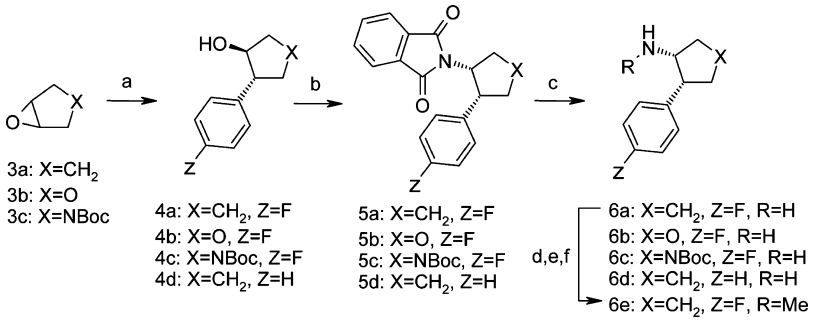

[a]Conditions: (a) 4-Z-PhMgBr, CuI, THF (Z = H or F); (b) phthalimide, diisopropyl azodicarboxylate, resin-bound PPh_3, THF; (c) anhydrous hydrazine, toluene, 90 °C (**6a**, **6b**, and **6d**) or hydrazine monohydrate, ethanol, 20 °C (**6c**); (d) Boc_2O, CH_2Cl_2; (e) NaH, MeI, DMF; (f) HCl.

Scheme 3. [a]

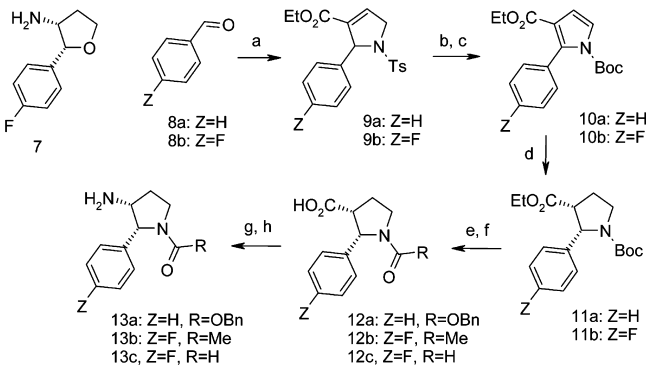

[a]Conditions: (a) $TsNH_2$, but-2-ynoic acid ethyl ester, PBu_3, BF_3-etherate, toluene, reflux; (b) KOtBu, THF; (c) Boc_2O, 4-DMAP; (d) PtO_2, H_2, 45 psi, ethanol; (e) HCl(aq), dioxane, 70 °C; (f) R = OBn, CbzCl, $NaHCO_3$; R = Me, Ac_2O; R = H; ethyl formate, 80 °C; (g) diphenylphosphoryl azide, triethylamine, toluene, 70 °C; then KOtBu, 20 °C; then Boc_2O; (h) HCl, dioxane, methylene chloride.

(**26**; see Table 1). During the hydrogenolysis of the adduct of **13a** and **1**, an over-reduced product was observed by LC/MS (mass plus two, product not identified), which lowered the overall yield. To avoid the low yield in the hydrogenolysis reaction when making the fluoro derivatives (**13b** and **13c**), the formyl and acetyl groups were installed before coupling to **1**, as shown in Scheme 3. The free amine analogue (**23**, Table 1) was made from the formyl derivative **24** by treating with aqueous hydrochloric acid in methanol at ambient temperature.

Single enantiomers were desired and were accessed by the separation of enantiomers using chiral SFC separation of intermediates before coupling to **1** or on the final analogues (see Experimental Section for details). The absolute stereochemistry of the most active enantiomer was determined by crystallization in PDK1 for several analogues (**18**, **20**, **21**, and **26**; see Figure 7 for one example), all of which showed the absolute stereochemistry as depicted in Schemes 2 and 3 and in Table 1 (see below).

RESULTS AND DISCUSSION

The PDK1 program began with a screen of selected compounds from the Pfizer corporate file. Of the resultant hits, the ligand efficient (LE)[19] inhibitor **14** (Figure 2) was selected for follow-up, including cocrystallization with PDK1. Analysis of the X-ray structure of **14** bound in PDK1 revealed a hydrogen bond between the carbonyl of the ligand and Thr-222. Analysis of the structure of ATP in PDK1 shows a hydrogen bond to Thr-222 through an intermediary water. The displacement of the water in the ATP/PDK1 structure could contribute to the high binding efficiency of **14**.[20] Various replacements for the isopropyl group were tried, but the more lipophilic groups (e.g., cyclobutyl, cyclopentyl, *sec*-butyl) were not significantly more potent, and the more polar groups (e.g., ethyl, hydroxyethyl, aminoethyl) lost 2-fold or more in potency (data not shown).

Since PI3K inhibition could itself reduce the amount of phospho-AKT and confound the analysis of inhibition of T308 phosphorylation due to PDK1, the program placed an emphasis on obtaining analogues selective against PI3Kα. Initial analogues afforded a few promising leads for building selective compounds such as the pyridyl-containing analogue **15** (Figure 3) with 7-fold selectivity against PI3K (in contrast, **14** only had 2-fold selectivity against PI3K). An analysis of the cocrystal structure led to hypotheses to improve both the potency in PDK1 and the selectivity against PI3K, as discussed below.

Figure 4 shows the cocrystal structure of **15** in PDK1. The substituents on the ethyl linker are in a gauche conformation (see lower right of Figure 4), rather than the usual anti conformation. The gauche conformation is necessary to efficiently fill the pocket under the G-loop of PDK1. To improve potency, we envisioned locking the flexible ethyl linker into a five-membered ring which would position the aryl ring under the G-loop and in the bioactive conformation. The pyridine ring was replaced with a phenyl ring because the nitrogen was not close enough to Ser-94 to make a significant hydrogen bond (3.3 Å) and because unblocked pyridines are associated with increased risk of CYP inhibition.[21] No loss in potency was anticipated because the phenyl analogue of **15** was equipotent (PDK1 K_i 29 nM).

Figure 5 shows **15** modeled into PI3K-γ.[22] Analysis of analogue **15** in PI3K-γ led to two hypotheses to improve the selectivity. First, substitution of the 4-position of the terminal aryl ring (pyridyl in **15**) with a fluorine was hypothesized to bump into Pro-810 in PI3K-γ. Second, methylation of the NH attached to the pyrazine was expected to bump into Ile-963. Both the fluorine and methyl groups were predicted to be at least tolerated by PDK1 and possibly beneficial to binding.

Figure 6 shows the dramatic improvement in potency and selectivity in the ring-locked analogue **17** compared to the open-chain analogue **15**. The ca. 15-fold increase in potency (ΔG = 1.6 kcal/mol) is consistent with the energy gain from freezing two rotatable bonds (est. 0.7 kcal/mol per rotatable bond) along with additional van der Waals interactions from one of the linker ring atoms (est. 0.8 kcal/mol per sp3 carbon).[23] Furthermore, in agreement with the predictions from the crystal structure, the selectivity against PI3Kα was

dx.doi.org/10.1021/jm201019k | J. Med. Chem. 2011, 54, 8490–8500

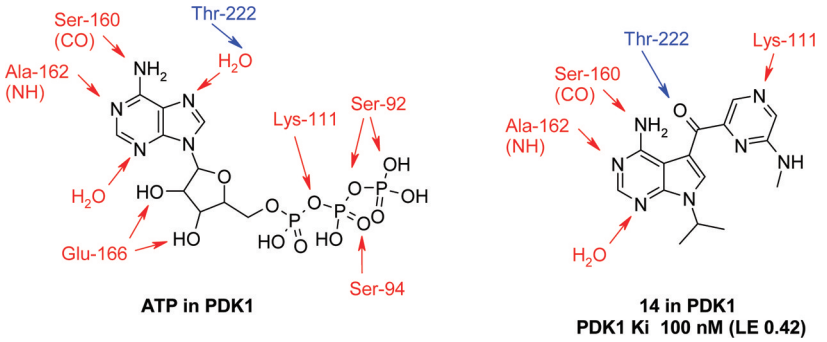

Figure 2. ATP and cmpd **14** shown with key interaction to PDK1 protein.

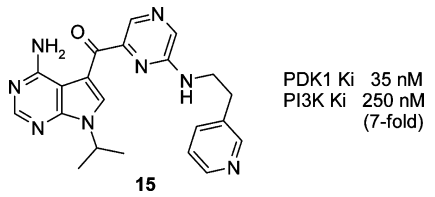

Figure 3. Early lead **15** with moderate selectivity against PI3K.

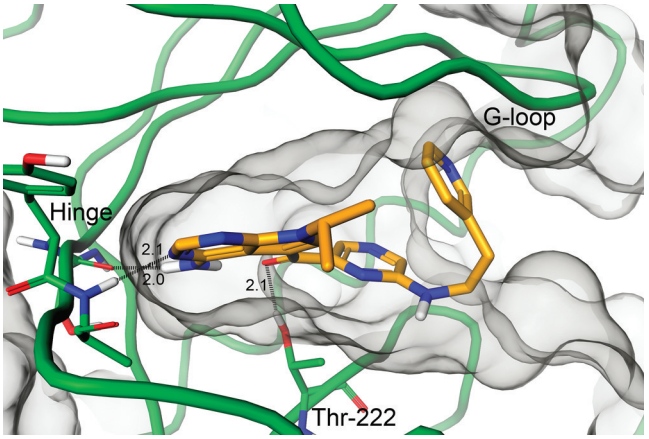

Figure 4. X-ray crystal structure of **15** (orange stick representation) bound to PDK1 (shown in green backbone trace).

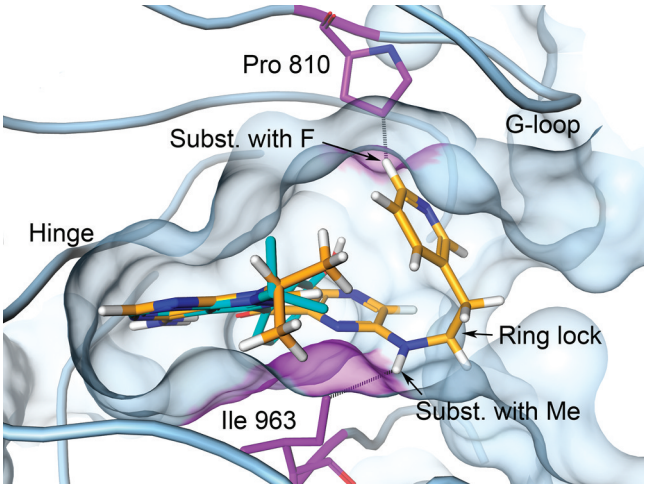

Figure 5. X-ray crystal structure of **16** (blue stick representation) bound to PI3K-γ[22] and analogue **15** (orange stick representation) modeled into the PI3K pocket by aligning the hinge binder.

improved by the substitution of a fluoro at the 4-position of the phenyl ring (**18**) and by methylation of the pyrazine-NH (**19**). Because the N-methylated analogue **19** showed N-demethylation as a major clearance pathway and because the potency and selectivity were not significantly different from those of the desmethyl analogue **18**, further analogues focused on the desmethyl series. The X-ray structures of ether analogue **20** (see Table 1 below for structure) and others (**18**, **21**, and **26**, data not shown) in PDK1 confirmed the expected placement of the aryl ring under the G-loop (see Figure 7).

Table 1 shows some in vitro ADME and selectivity data for the cyclopentyl linker analogue **18**. This analogue has poor

Table 1. In Vitro ADME and Selectivity for Ring-Locked Analogues[a]

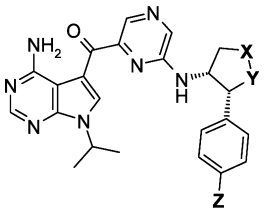

						in vitro ADME				Selectivity[f]			
#	X	Y	Z	clogP	PDK1 Ki (nM)	CYP % Inh.[b]	Solubility[c]	Permeability[d]	HLM Cl[e]	PI3K (nM)	S6K (nM)	AKT (nM)	mTOR (nM)
18	CH_2	CH_2	F	4.6	1.0	85	6	6	160	470	230	210	3900
20	O	CH_2	F	2.9	0.6	53	23	13	160	570	170	260	500
21	CH_2	O	F	2.9	1.3	23	120	13	220	430	61	230	3900
22	NH	CH_2	F	2.8	2.5	27	480	2	59	370	11	10	1100
23	CH_2	NH	F	2.8	1.0	27	520	5	92	150	120	100	2100
24	CH_2	NCHO	F	2.4	0.7	38	290	11	62	130	890	170	2800
25	CH_2	NAc	F	2.3	1.4	37	390	11	120	1300	10000	360	2600
26	CH_2	NAc	H	2.1	1.4	54	510	11	110	1900	3600	1100	3900

[a]All compounds are single enantiomers with ≥95% ee. [b]% inhibition at 3 uM; maximum value from CYP-1A2, -2C9, -2D6, and -3A4; the most strongly inhibited enzyme was CYP-3A4 in all cases in the table. [c]Solubility tested at Analiza,[25] pH 6.5, in μM. [d]Passive permeability in canine kidney cells, $\times 10^{-6}$ cm/s. [e]Human liver microsome clearance, μL/(min mg). [f]K_i against kinase shown: green, >100 nM; yellow, 30–100 nM; red, <30 nM.

dx.doi.org/10.1021/jm201019k | J. Med. Chem. 2011, 54, 8490–8500

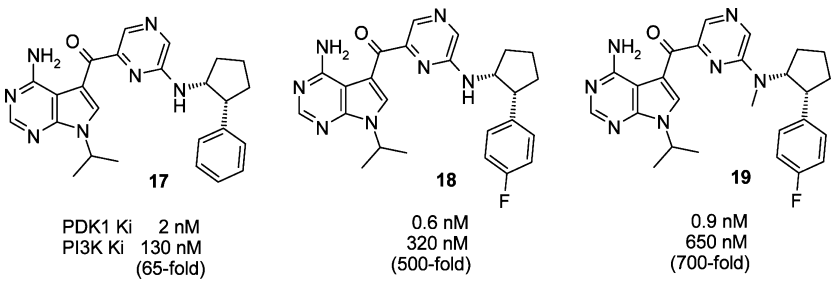

Figure 6. Ring-locked derivatives of **15**.

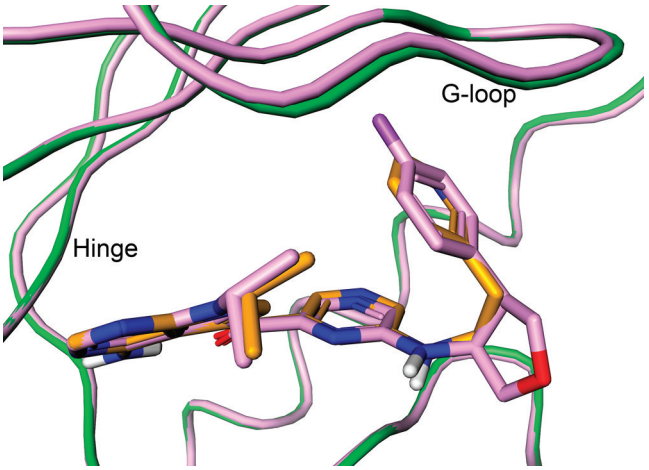

Figure 7. Superposition of the X-ray crystal structures of PDK1 bound to **15** (orange sticks/green backbone trace) and **20** (pink sticks and backbone trace).

solubility, high clearance, and high CYP3A4 inhibition, likely arising in part due to the compound's high lipophilicity.[24] Further designs targeted analogues with clogP < 3 to improve the overall probability of favorable ADME properties. Because the 4-fluorophenyl ring demonstrated good selectivity against PI3K, that moiety was left intact and the lipophilicity was lowered by replacing the methylenes in the cyclopentyl ring with heteroatoms. Further SAR on replacements for the 4-fluorophenyl ring will be reported in a future publication.

Replacement of the cyclopentyl ring with two isomeric tetrahydrofuran rings gave analogues **20** and **21**, lowering the clogP by 1.7 units. The PDK1 potency was maintained while the permeability and solubility improved in both cases. Isomer **21** also reduced the CYP inhibition although the selectivity against S6K was reduced in this analogue to ca. 50-fold.

Substitution of the methylenes with nitrogen gave the basic pyrrolidine analogues **22** and **23**, which lowered the clogP by about the same degree as that for the ethers (measured LogD values at pH 7.4 were 1.7 and 2.4, respectively). Once again, the PDK1 potency was maintained. While the solubility and CYP inhibition were good, the passive permeability suffered, possibly from a desolvation penalty of the basic amines. The selectivities for these two isomers were dramatically different, with **22** becoming more potent against S6K and AKT.

Formylation and acetylation of the basic amine in **23** gave **24** and **25**, respectively. These analogues reduced the clogP by more than 2 units from **18** while maintaining potency. As expected for analogues in this clogP range, the solubility, CYP inhibition, and permeability were moderate to good; however, the HLM clearance was still high. The additional polarity did not adversely affect the permeability, and both analogues had excellent selectivity against all the PI3K-pathway kinases in the panel. Compound **24** improved the potency over 100-fold from **14** and has an LE of 0.38.[26]

Since the acetyl group in analogue **25** gave a boost in selectivity over the formyl group in **24**, the des-fluoro analogue of **25** was made to see if selectivity could be maintained against PI3K and the other pathway kinases. Indeed, the des-fluoro analogue **26** maintained potency and selectivity. The in vitro ADME was similar to **25** with the exception of higher CYP inhibition (54% at 3 μM against CYP3A4).

The in vitro cellular potencies (reduction of pAKT-T308) for analogues **24**–**26** are shown in Table 2. The two fluorinated pyrrolidine amide analogues, **24** and **25**, showed good potency in two different cell lines. The des-fluoro analogue **26** was less potent in the cell assay. The approximate 100-fold shift between K_i and cellular IC_{50} was consistent with the analogues in this series.

Table 2. In Vitro Cellular Potency

		cell IC_{50}[a] (nM) ± std dev	
cmpd	PDK1 K_i (nM)	SKOV3	A549
24	0.7	70 ± 30 (n = 8)	50 ± 20 (n = 2)
25	1.4	70 ± 40 (n = 6)	80 ± 10 (n = 2)
26	1.4	200 ± 50 (n = 5)	300 ± 130 (n = 2)

[a]Inhibition of pAKT-T308 using the ELISA assay in the tumor cell lines SKOV3 or A549.

To assess broader selectivity, analogues **24**–**26** were profiled against a larger panel of kinases from Invitrogen (kinases inhibited at 70% or more are shown in Table 3; see Supporting Information for results from the full panel of 36 kinases). Both compounds with the 4-fluoro substituent (**24** and **25**) inhibited five other kinases at >70% at 1 μM, while the des-fluoro analogue **26** only inhibited one other kinase (Chk2) above 70%.

Table 3. Kinases Inhibited at >70% at 1 μM

	% inhibition at 1 μM[a]		
gene/kinase	cmpd **24**	cmpd **25**	cmpd **26**
CHEK2/Chk2	98	99	94
MARK1	84	74	47
STK6/Aurora A	81	80	54
NTRK1/TrkA	74	63	59
PRKACA	74	58	30
GSK3β	66	76	42
CAMK2A	62	73	32

[a]All values an average of n = 2 or greater.

Because activity against the kinases MARK1, Aurora A, TrkA, and GSK3β might contribute to antiproliferative effects in

dx.doi.org/10.1021/jm201019k | J. Med. Chem. 2011, 54, 8490–8500

culture and confound the interpretation of the results for PDK1 inhibition, the IC_{50} values for these kinase were measured (Table 4). While all three analogues are greater than 100-fold

Table 4. IC_{50} against Off-Target Kinases

	IC_{50} for kinase (nM)		
kinase	cmpd **24**	cmpd **25**	cmpd **26**
AurA	140	460	820
GSK3β	180	340	860
MARK1	110	590	1300
TrkA	200	620	910

selective against these four kinases, analogues with the acetamide group (**25** and **26**) are more selective than the formamide analogue (**24**). A potency of *ca.* 100 nM for **24** against Aurora A, MARK1, and PI3K (Table 1) could potentially contribute to moderate activity in an antiproliferation assay, whereas there is less concern with analogues **25** and **26**.

The antiproliferative activity for **24**–**26** was measured in two tumor cell lines, A549 and H460 (Table 5). In A549, even though good levels of pAKT-T308 reduction are observed, the levels of antiproliferative activity were modest at best with 20- to 30-fold increase between IC_{50} and EC_{50}. In the H460 cell line, lower reductions in pAKT-T308 levels were seen with similar levels of antiproliferative activity, resulting in a lower fold increase between IC_{50} and EC_{50} (*ca.* 5-fold). The modest growth inhibition in H460 for these selective PDK1 inhibitors was disappointing considering that both a PI3K-selective inhibitor[27] and an mTOR-selective inhibitor[28] had an EC50 ca. 100 nM in the same cell line.

In summary, we have discovered potent inhibitors of PDK1 with excellent selectivity within the pathway (PI3K, AKT, S6K, and mTOR) and against a broader range of kinases. The PI3K selectivity was achieved by filling under the G-loop, and the solubility, permeability, and CYP liability were improved by lowering the lipophilicity of the selective lead **18**. While the potent and selective PDK1 inhibitors effectively reduced pAKT-T308 in tumor cells in vitro, they had only modest effects in preventing tumor cell growth in the in vitro antiproliferation assay.

EXPERIMENTAL SECTION

Reagents and General Enzymatic Assay Conditions. EDTA, Tris, and Hepes buffer, DMSO, ATP, DTT, magnesium chloride, Brij-35, and Triton X-100 were purchased from Sigma-Aldrich (St Louis, MO). Fluorescent labeled AKT substrate (5FAM-GRPRTSSFAEG-CONH2) and S6K substrate (5FAM-KRSRTRTDSYSAGQ-COOH, respectively) were purchased from Caliper LifeSciences (Hopkinton, MA) and CPC Scientific (San Jose, Ca), respectively. The PDK1 Omnia peptide (Ac-Sox-PKTFCGTPEYLAPEVRREPRILSEEE-QEMFRDFDYIAD-NH_2) was purchased from Invitrogen Life Technologies (Carlsbad, CA). The recombinant GST-tagged P70S6K (a.a. 1-421), His-tagged AKT1 (full length), and GST-tagged mTOR (a.a. 1360-2549) were purchased from Invitrogen. Recombinant human His-tagged PDK1 catalytic domain (a.a. 51-359) was made in-house at Pfizer La Jolla.[29]

All the kinetic experiments were conducted at room temperature (~22 °C), and the concentrations of reagents reported in the following sections are reported as final in the media buffer. All the experimental data were generated in duplicate and were fitted using nonlinear regression analysis software, GraphPad Prism 5.[30]

Selectivity Screening against Kinase Panel. K_i values were determined for AKT1 and P70S6K (S6K), using a Caliper EZ-reader instrument from Caliper LifeScience. For AKT1, kinetic studies were conducted in the presence of 2.2 nM enzyme, 20 μM ATP, 5 μM 5FAM-peptide in a 100 mM Hepes pH 7.4, 10 mM $MgCl_2$, 0.003% Brij35, 1 mM DTT assay buffer at pH 7.4. The substrate and product were separated on the basis of charge using upstream, downstream voltages of −2800 V, −380 V, respectively, and a screening pressure of 0.8 psi. For S6K, kinetic studies were conducted in the presence of 5 nM enzyme, 50 μM ATP, 5 μM 5FAM-peptide in a 20 mM Tris·HCl, 15 mM $MgCl_2$, 50 mM NaCl, 0.1 mM EDTA, 1 mM DTT assay buffer at pH 7.4. The substrate and product were separated using upstream and downstream voltages of −2500 V and −500 V, respectively, and a screening pressure of −1.2 psi. For PDK1, kinetic studies were conducted in the presence of 20 nM enzyme, 50 μM ATP, and 3 μM Sox-peptide in a 50 mM Hepes, 5 mM $MgCl_2$, 0.01% Brij35, 1 mM DTT assay buffer at pH 7.4. The increase of fluorescence (λ_{ex} = 360 nm and λ_{em} = 485 nm) was recorded using a Safire TECAN plate reader. For mTOR, an in vitro LanthaScreen kinase assay (Invitrogen - Life Technologies) was conducted to determine the level of phosphorylation of the protein substrate 4E-BP1 at Thr46 in a TR-FRET format. The phosphorylation of GFP-4E-BP1 at Thr46 is recognized by the Terbium-anti-p4E-BP1 antibody, which results in time-resolved fluorescence resonance energy transfer (TR-FRET) between GFP and terbium in the antibody–product complex. Kinetic studies were conducted in the presence of 1 nM mTOR, 0.4 μM GFP-4E-BP1, 2 mM antibody (added at the end of the reaction), 40 μM ATP in a 50 mM Hepes, 10 mM $MgCl_2$, 1 mM EGTA, 0.01% Tween-20, assay buffer at pH 7.4. For PI3Kα, the kinase reaction mixture (i.e. 0.5 nM mouse PI3Kα diluted in assay buffer, 30 μM PIP_2, compound, 5 mM $MgCl_2$, and 200 μM ATP) was incubated for 30 min prior to adding EDTA (10 mM) to stop the reaction. The mixture was added to the Detector/Probe mix containing 480 nM GST-Grp1 PH Domain and 12 nM TAMRA tagged fluorescent PIP_3 dissolved in assay buffer for 3 min. Polarization (mP) values decreased as TAMRA tagged PI(3,4,5)P_3 probe binding to the GST-Grp1 PH domain was displaced by PIP_3 produced by the PI3Kα enzymatic reaction. Polarization of fluorescence studies were conducted in a 50 mM Hepes pH 7.4, 150 mM NaCl, 5 mM DTT, and 0.05% CHAPS.

The data from the broad kinase selectivity panel were provided by Invitrogen as fee-for-service and were generated in the presence of 1 μM of inhibitor against a panel of 35 selected kinases.

K_i Determination. K_i^{app} and K_i were calculated by fitting the experimental data to the following equations:[31]

Table 5. In Vitro Cellular Potency in Biomarker and Functional Assays

		A549 (nM)			H460 (nM)		
cmpd	PDK1 K_i (nM)	pAKT[a] IC_{50}	proliferation[b] EC_{50}	fold shift[c]	pAKT[a] IC_{50}	proliferation[b] EC_{50}	fold shift[c]
24	0.7	50	1800	36	120	700	6
25	1.4	80	2200	28	160	1900	12
26	1.4	300	5200	17	320	1700	5

[a]ELISA pAKT-T308 inhibition assay. See Table 2 for statistics. [b]Cell proliferation assay using resazurin, n = 2, individual values within 30% of average. [c]Proliferation EC_{50}/pAKT IC_{50}.

dx.doi.org/10.1021/jm201019k | J. Med. Chem. 2011, 54, 8490–8500

$$V_i = V_o\left(1 - \left(\left\{[E]_o + [I]_o + K_i^{app} - \sqrt{([E]_o + [I]_o + K_i^{app})^2 - 4[E]_o[I]_o}\right\}/2[E]_o\right)\right) \quad (1)$$

where

$$K_i^{app} = K_i(1 + [A_o]/K_m) \quad (2)$$

$[E]_o$ and $[I]_o$ are the total active enzyme and inhibitor concentrations, respectively; K_i is the inhibition binding constant; V_i and V_o are the rates of peptide phosphorylation in the presence or in the absence of inhibitor, respectively; $[A]_o$ is the total ATP concentration.

pAKT-T308 ELISA Assay. Cells were plated at 50,000 cells/well in a 96-well microtiter plate and allowed to adhere overnight. Inhibitor compounds were added to each well (3-fold serial dilution, range 0.0169 nM to 10 μM) for 2 h prior to cell lysis. After compound treatment, cells were lysed and lysate transferred to the ELISA plate. The pAKT T308 ELISA was performed per the manufacturer's directions (Cell Signaling Technology). All assays were run in duplicate and have been repeated at least twice.

Cell Proliferation Assay. Cells were plated at 3,000 cells/well in a 96-well microtiter plate and allowed to adhere overnight. Inhibitor was added to each well (3-fold serial dilution, range 0.0169 nM to 10 μM) and incubated. At 72 h postcompound addition, 250 μg/mL of resazurin was added to all wells. Plates were incubated at 37 °C for an additional 6 h followed by capture of the fluorescence signal using emission 590 nm and excitation 560 nm. All assays were run in duplicate and have been repeated at least twice.

General Chemistry Experimental. All reagents and solvents were used as purchased from commercial sources. Flash chromatography was run on ISCO or Biotage compatible silica gel cartridges and eluted with ethyl acetate in heptane unless otherwise noted. All reactions were performed under a positive pressure of nitrogen, at ambient temperature, and in anhydrous solvents, unless otherwise indicated. Microwave assisted reactions were run in a Smith Creator (Personal Chemistry). ^{1}H NMR spectra were recorded on a Bruker instrument operating at 300 or 400 MHz as indicated. The mass spectra were obtained using liquid chromatography mass spectrometry (LC-MS) on an Agilent instrument using atmospheric pressure chemical ionization (APCI) or electrospray ionization (ESI). All test compounds showed >95% purity as determined by combustion analysis. Combustion analyses were performed by Atlantic Microlab, Inc. (Norcross, GA). Chiral SFC separations were run on a 21.2 mm × 250 mm column at 100 bar, 35 °C, and 60−65 mL/min unless otherwise noted.

General Procedure for Final Compounds (2). A mixture of (4-amino-7-isopropyl-7H-pyrrolo[2,3-*d*]pyrimidin-5-yl)-(6-chloropyrazin-2-yl)methanone (**1**) (100 mg, 0.32 mmol), primary or secondary amine (0.47 mmol), cesium fluoride (146 mg, 0.96 mmol), and Hunig's base (165 mg, 1.3 mmol) in anhydrous DMSO (1.2 mL) was heated at 120 °C for 16 h. The crude was filtered to remove salts and purified by reverse phase HPLC to provide title compounds as yellow solids.

(*trans*)-3-(4-Fluorophenyl)-4-hydroxypyrrolidine-1-carboxylic Acid *tert*-Butyl Ester (4c). A solution of 6-oxa-3-aza-bicyclo[3.1.0]-hexane-3-carboxylic acid *tert*-butyl ester (**3c**, 2.0 g, 11 mmol) in 2-Me-THF (5 mL) was added dropwise to a solution of the 4-fluorophenylmagnesium bromide (2.0 M in THF, 11 mL, 22 mmol) and copper iodide (100 mg, 0.54 mmol) at 0 °C. The reaction was allowed to warm to 20 °C and stirred for 16 h. The reaction was cooled to 0 °C and quenched with sat. aq ammonium chloride. The product was extracted with ethyl acetate. The organics were washed with sodium bicarbonate and brine, dried over sodium sulfate, and concentrated in vacuo. The crude was purified by flash chromatography to give the title compound **4c** as a yellow oil (2.1 g, 69%). ^{1}H NMR (400 MHz, $CDCl_3$) δ ppm 1.49 (s, 9 H), 2.02 (br s, 1 H), 3.24 (q, J = 7.6 Hz, 1 H), 3.31 (dd, J = 11.5, 5.7 Hz, 1 H), 3.48 (dd, J = 11.3, 7.6 Hz, 1 H), 3.76 (dd, J = 11.3, 6.3 Hz, 1 H), 3.88 (dd, J = 11.1, 7.8 Hz, 1 H), 4.29 (q, J = 6.3 Hz, 1 H), 7.00−7.07 (m, 2 H), 7.19−7.25 (m, 2 H). LC-MS (APCI$^+$) 182 (M + H-Boc).

***cis*-3-(1,3-Dioxo-1,3-dihydroisoindol-2-yl)-4-(4-fluorophenyl)pyrrolidine-1-carboxylic Acid *tert*-Butyl Ester (5c).** To a solution of alcohol **4c** (2.1 g, 7.5 mmol), phthalimide (1.3 g, 9 mmol), and triphenylphosphine (2.4 g, 9 mmol) at 0 °C was added slowly diisopropyl azodicarboxylate (1.9 g, 9 mmol). The reaction mixture was allowed to warm to 20 °C and was stirred for 16 h. The solution was concentrated in vacuo, dissolved in ethyl acetate, washed with 2 M aqueous sodium hydroxide and brine, dried over sodium sulfate, and concentrated in vacuo. The crude was purified by flash chromatography to give the title compound **5c** as a white solid (2.6 g, 85%). ^{1}H NMR (400 MHz, $CDCl_3$) δ ppm 1.54 (s, 9 H), 3.76−3.87 (m, 1 H), 3.87−4.09 (m, 3 H), 4.99 (spt, J = 6.2 Hz, 1 H), 5.11 (td, J = 7.6, 4.0 Hz, 1 H), 6.79−6.86 (m, 2 H), 7.11 (dd, J = 8.4, 5.4 Hz, 2 H), 7.63−7.68 (m, 2 H), 7.68−7.73 (m, 2 H). LC/MS (APCI$^+$): 311 (M + H-Boc).

***cis*-3-Amino-4-(4-fluorophenyl)pyrrolidine-1-carboxylic Acid *tert*-Butyl Ester (6c).** A solution of phthalimide **5c** (2.6 g, 6.4 mmol) and hydrazine monohydrate (3.25 g, 64 mmol) in ethanol (30 mL) was stirred at 20 °C for 3 days. The reaction was concentrated from ethanol 3-times to remove excess hydrazine. The residue was dissolved in ethyl acetate and filtered to remove solids. The filtrate was absorbed onto an SCX column and rinsed with methanol. The product was eluted with 3.5 M ammonia in methanol. The eluent was concentrated in vacuo to give the title compound **6c** as a yellow oil (1.3 g, 71%). ^{1}H NMR (400 MHz, $CDCl_3$) δ ppm 1.50 (s, 9 H), 3.18−3.32 (m, 1 H), 3.38 (td, J = 7.8, 5.3 Hz, 1 H), 3.49 (s, 2 H), 3.58−3.83 (m, 4 H), 7.02−7.09 (m, 2 H), 7.20 (d, J = 5.3 Hz, 2 H). LC-MS (APCI$^+$) 181 (M + H-Boc).

***cis*-2-(4-Fluorophenyl)tetrahydrofuran-3-ylamine (7).** Synthesized following the procedure from Andreotti and Ward[17] for the analogous des-fluoro compound. ^{1}H NMR (300 MHz, MeOH-d_4) δ ppm 2.62−2.81 (m, 1 H), 3.03−3.22 (m, 1 H), 4.41−4.56 (m, 1 H), 4.56−4.67 (m, 1 H), 4.73−4.90 (m, 1 H), 5.52 (d, J = 3.8 Hz, 1 H), 7.60−7.79 (m, 2 H), 7.94−8.12 (m, 2 H). LC-MS (APCI$^+$) 182 (M + H).

Ethyl 2-(4-Fluorophenyl)-1-[(4-methylphenyl)sulfonyl]-2,5-dihydro-1H-pyrrole-3-carboxylate (9b). A solution of 4-fluorobenzaldehyde (15.2 g, 122 mmol), toluene-4-sulfonamide (20.9 g, 122 mmol), and borontrifluoride-etherate (0.45 g, 3.2 mmol) in anhydrous toluene (200 mL) was heated at reflux with a Sean−Stark trap for 4 h. The solution was allowed to cool to 20 °C. To the solution was added ethyl 2-butynoate (14.4 g, 128 mmol) and tri-*n*-butylphosphine (1.2 g, 6.1 mmol), and the solution was heated at 100 °C for 1 h. The solution was concentrated in vacuo to give a reddish-brown oil which was purified by flash chromatography to give the title compound **9b** (34.3 g, 72%). ^{1}H NMR (400 MHz, $CDCl_3$) δ ppm 1.12 (t, J = 7.1 Hz, 3 H), 2.39 (s, 3 H), 3.98−4.11 (m, 2 H), 4.33−4.45 (m, 1 H), 4.45−4.57 (m, 1 H), 5.67−5.77 (m, 1 H), 6.75−6.83 (m, 1 H), 6.93 (t, J = 8.6 Hz, 2 H), 7.12−7.24 (m, 4 H), 7.45 (d, J = 8.3 Hz, 2 H). LC/MS (APCI$^+$): 390 (M + H).

1-*tert*-Butyl 3-Ethyl 2-(4-Fluorophenyl)-1H-pyrrole-1,3-dicarboxylate (10b). To a solution of tosylate **9b** (17.2 g, 44 mmol) in anhydrous dimethylformamide (200 mL) at 0 °C was added dropwise a solution of potassium *tert*-butoxide in tetrahydrofuran (1.0 M, 46 mL, 46 mmol) over 1.5 h. The solution was then allowed to warm to 20 °C over 30 min and stirred at 20 °C for 1.5 h. To the solution of pyrrole was added Boc anhydride (19.2 g, 88 mmol) and 4-dimethylaminopyridine (110 mg, 0.9 mmol). The solution was stirred at 20 °C for 2 h. The tetrahydrofuran was removed in vacuo. The residue was diluted with saturated aqueous ammonium chloride (500 mL) and extracted with diethyl ether (400 mL). The organics were washed with brine (200 mL), dried with magnesium sulfate, and concentrated in vacuo. The crude was purified by flash chromatography to give the title compound **10b** (12.7 g, 86%). ^{1}H NMR (400 MHz, $CDCl_3$) δ ppm 1.12 (t, J = 7.1 Hz, 3 H), 1.30 (s, 9 H), 4.09 (q, J = 7.1 Hz, 2 H), 6.68 (d, J = 3.3 Hz, 1 H), 7.09 (t, J = 8.7 Hz, 2 H), 7.24−7.31 (m, 2 H), 7.33 (d, J = 3.5 Hz, 1 H). LC/MS (APCI$^+$): 334 (M + H).

1-*tert*-Butyl 3-Ethyl (2*S*,3*R*)-2-(4-Fluorophenyl)pyrrolidine-1,3-dicarboxylate (11b). A mixture of pyrrole **10b** (12.7 g, 38 mmol) and platinum(IV) oxide (7.5 g, 55 mmol) in ethanol (200 mL) was shaken in a Parr shaker with 45 psi hydrogen at 20 °C for 24 h. The catalyst was removed by filtering through Celite and rinsing with ethanol. CAUTION: Care must be taken to not let the filter cake go dry to avoid a fire. The filtrate was concentrated in vacuo to give the title compound **11b** (12.1 g, 94%). ^{1}H NMR (400 MHz, $CDCl_3$) δ ppm 1.04 (t, J = 7.2 Hz, 3 H), 1.19 (s, 6 H), 1.37−1.49 (m, 3 H), 2.02−2.13 (m, 1 H), 2.34−2.49 (m, 1 H), 3.31−3.45 (m, 1 H), 3.45−3.58 (m, 1 H), 3.76−3.82 (m, 1 H), 3.87 (m, 2 H), 5.01−5.24 (m, 1 H), 6.92−7.00 (m, 2 H), 7.06−7.17 (m, 2 H). LC/MS (APCI$^+$): 238 (M + H-Boc).

***cis*-1-Acetyl-2-(4-fluorophenyl)pyrrolidine-3-carboxylic Acid (12b).** A solution of ester **11b** (12.1 g, 36 mmol) in dioxane (100 mL) and aqueous 6 N hydrochloric acid (100 mL) was heated at 70 °C for 40 h. The solution was cooled to 0 °C, and solid sodium bicarbonate was added slowly and carefully until the final pH was 8. To the solution was added acetic anhydride (11 g, 107 mmol), and the solution was stirred at 20 °C for 3.5 h. The solution was cooled to 0 °C, and aqueous 6 N hydrochloric acid was added dropwise to lower the pH to 2. The aqueous solution was extracted with methyl *tert*-butyl ether. The organics were washed with brine, dried with magnesium sulfate, and concentrated in vacuo. The oil was reconcentrated from heptane and ethyl acetate to give a light yellow solid. The solid was triturated with heptane (ca. 250 mL) using vigorous stirring, collected by vacuum filtration, and rinsed with heptane to give a white solid which was dried overnight at 40 °C under high vacuum to give the title compound **12b** (8.4 g, 93%). ^{1}H NMR (400 MHz, DMSO-d_6, 1:1 mixture of rotamers A:B) δ ppm 1.67 (s, 1.5 H, rotamer A), 1.98 (s, 1.5 H, rotamer B), 1.91−2.07 (m, 1 H), 2.07−2.29 (m, 1 H), 3.34−3.62 (m, 2 H), 3.70−3.82 (m, 0.5 H, rotamer A), 3.91 (t, J = 9.1 Hz, 0.5 H, rotamer B), 5.18 (d, J = 8.3 Hz, 0.5 H, rotamer A), 5.26 (d, J = 8.6 Hz, 0.5 H, rotamer B), 7.00−7.11 (m, 1 H, rotamer A), 7.11−7.27 (m, 2 H plus 1 H, rotamer B), 12.33 (br s, 1 H). LC/MS (APCI$^+$): 252 (M + H).

***cis*-2-(4-Fluorophenyl)-1-formylpyrrolidine-3-carboxylic Acid (12c).** A solution of ester **11b** (9.15 g, 27 mmol) in dioxane (60 mL) and aqueous 6 N hydrochloric acid (53 mL) was heated at 70 °C for 2 days. The solution was cooled to 0 °C, and solid sodium bicarbonate was added slowly and carefully until the final pH was 8. To the solution was added ethyl formate (54 mL, 675 mmol), and the reaction mixture was heated at 80 °C for 40 h. The reaction was cooled to about 0 °C and acidified to pH 1 using 6 N aqueous hydrochloric acid (ca. 30 mL). The product was extracted with ethyl ether (600, 300, and 200 mL). The combined organics were dried over sodium sulfate and concentrated in vacuo to give the title compound **12c** (5.87 g, 92%). ^{1}H NMR (400 MHz, DMSO-d_6, 1.6:1 mixture of rotamers A:B) δ ppm 1.94−2.09 (m, 1 H), 2.09−2.25 (m, 1 H), 3.36−3.48 (m, 1 H plus 0.6 H, rotamer A), 3.65 (td, J = 9.8, 7.3 Hz, 0.4 H, rotamer B), 3.70−3.78 (m, 0.6 H, rotamer A), 3.98 (td, J = 9.2, 2.8 Hz, 0.4 H, rotamer B), 5.16 (d, J = 8.3 Hz, 0.4 H, rotamer B), 5.34 (d, J = 8.3 Hz, 0.6 H, rotamer A), 7.04−7.26 (m, 4 H), 8.07 (s, 0.6 H, rotamer A), 8.21 (s, 0.4 H, rotamer B), 12.39 (br s, 1 H). LCMS (APCI$^+$): 238 (M + H).

***cis*-1-[3-Amino-2-(4-fluorophenyl)pyrrolidin-1-yl]ethanone Hydrochloride Salt (13b).** A solution of acid **12b** (8.2 g, 33 mmol), triethylamine (5.0 g, 49 mmol), and diphenylphosphoryl azide (12.5 g, 45 mmol) in toluene (1100 mL) was heated at 70 °C for 4 h. The solution was cooled to 20 °C, 1.0 M potassium *tert*-butoxide solution in tetrahydrofuran (68 mL, 68 mmol) was added, and the resulting mixture was stirred at 20 °C for 20 min. Boc anhydride (12 g, 55 mmol) and 4-dimethylaminopyridine (200 mg, 1.6 mmol) were added, and the mixture was stirred at 20 °C for 16 h. The solution was washed with saturated aqueous ammonium chloride solution (2 × 600 mL) and brine (500 mL), dried with magnesium sulfate, and concentrated in vacuo. The crude was purified by flash chromatography to give *cis*-*tert*-butyl [1-acetyl-2-(4-fluorophenyl)pyrrolidin-3-yl]carbamate (5.3 g, 50%, 16 mmol), which was dissolved in a solution of anhydrous methylene chloride (160 mL) and 4 M hydrochloric acid in dioxane (23 mL, 92 mmol), and the solution was stirred at 20 °C for 18 h. The solvent was removed in vacuo, and the white solid was dried under high vacuum at 50 °C to give the title compound **13b** (4.3 g, 100%). ^{1}H NMR (400 MHz, DMSO-d_6, 1.3:1 mixture of rotamers A:B) δ ppm 1.66 (s, 1.3 H, rotamer B), 1.77−1.97 (m, 1 H), 2.00 (s, 1.7 H, rotamer A), 2.13−2.30 (m, 1 H), 3.38−3.51 (m, 0.4 H, rotamer B), 3.58−3.68 (m, 0.6 H, rotamer A), 3.73−3.88 (m, 1 H), 3.88−4.02 (m, 1 H), 5.18 (d, J = 7.3 Hz, 0.6 H, rotamer A), 5.17 (d, J = 7.3 Hz, 0.4 H, rotamer B), 7.15−7.31 (m, 2 H), 7.31−7.44 (m, 2 H), 8.10 (br s, 1.7 H, rotamer A), 8.19 (br s, 1.3 H, rotamer B). LC/MS (APCI$^+$) 223 (M + H).

[4-Amino-7-(propan-2-yl)-7H-pyrrolo[2,3-*d*]pyrimidin-5-yl][6-(methylamino)pyrazin-2-yl]methanone (14). ^{1}H NMR (400 MHz, $CDCl_3$) δ ppm 1.56 (d, J = 6.8 Hz, 6 H), 3.12 (d, J = 5.1 Hz, 3 H), 4.81 (br s, 1 H), 5.11 (quin, J = 6.8 Hz, 1 H), 8.12 (s, 1 H), 8.34 (s, 1 H), 8.53 (s, 1 H), 8.75 (s, 1 H). LC/MS (ESI$^+$): 312 (M + H). Anal. Calcd for $C_{15}H_{17}N_7O{\cdot}2.85H_2O$: C, 49.92; H, 5.99; N, 26.71. Found: C, 49.67; H, 6.31; N, 27.03.

[4-Amino-7-(propan-2-yl)-7H-pyrrolo[2,3-*d*]pyrimidin-5-yl](6-{[2-(pyridin-3-yl)ethyl]amino}pyrazin-2-yl)methanone (15). ^{1}H NMR (400 MHz, $CDCl_3$) δ ppm 1.47 (d, J = 6.6 Hz, 6 H), 3.03 (t, J = 7.1 Hz, 2 H), 3.72−3.84 (m, 2 H), 4.85 (t, J = 5.7 Hz, 1 H), 5.07 (quin, J = 6.8 Hz, 1 H), 7.22−7.27 (m, 1 H), 7.51−7.58 (m, 1 H), 8.09 (s, 1 H), 8.34 (s, 1 H), 8.48−8.57 (m, 4 H). LC/MS (APCI$^+$): 403 (M + H). Anal. Calcd for $C_{21}H_{22}N_8O{\cdot}1.4H_2O$: C, 59.10; H, 5.73; N, 26.07. Found: C, 58.98; H, 5.84; N, 26.20.

[4-Amino-7-(propan-2-yl)-7H-pyrrolo[2,3-*d*]pyrimidin-5-yl](6-{[(1*R*,2*R*)-2-phenylcyclopentyl]amino}pyrazin-2-yl)-methanone (17). Enantiomers were separated on a Chiracel OD-H column with 30% methanol, 70% CO_2; the more active enantiomer eluted first and is the (+) isomer. ^{1}H NMR (400 MHz, DMSO-d_6) δ ppm 1.51 (d, J = 6.8 Hz, 3 H), 1.55 (d, J = 6.8 Hz, 3 H), 1.66−1.89 (m, 2 H), 1.90−2.04 (m, 1 H), 2.03−2.19 (m, 3 H), 3.37−3.47 (m, 1 H), 4.55−4.67 (m, 1 H), 5.01 (quin, J = 6.8 Hz, 1 H), 7.08 (dq, J = 8.6, 4.2 Hz, 1 H), 7.12−7.20 (m, 5 H), 7.46 (br s, 1 H), 7.97 (s, 1 H), 8.10 (s, 1 H), 8.22 (s, 1 H), 8.36 (br s, 1 H), 8.80 (s, 1 H). LC/MS (ESI$^+$): 442 (M + H). Anal. Calcd for $C_{25}H_{27}N_7O{\cdot}0.50H_2O$: C, 66.82; H, 6.20; N, 21.62. Found: C, 66.65; H, 6.26; N, 21.76.

(4-Amino-7-isopropyl-7H-pyrrolo[2,3-*d*]pyrimidin-5-yl)-{6-[(1*R*,2*R*)-2-(4-fluorophenyl)cyclopentylamino]pyrazin-2-yl}-methanone (18). Single enantiomers were obtained by separating the N-Boc derivative of **6a** using a Chiralpak AD-H column eluting with 9% methanol and 91% CO_2; the desired enantiomer eluted first and had optical rotation $[\alpha]_D^{22}$ +47 (*c* 0.25, MeOH). The Boc group was removed with HCl before coupling to **1**. ^{1}H NMR (400 MHz, DMSO-d_6) δ ppm 1.48 (d, J = 6.8 Hz, 3 H), 1.53 (d, J = 6.6 Hz, 3 H), 1.62−1.86 (m, 2 H), 1.86−2.18 (m, 4 H), 3.35−3.45 (m, 1 H), 4.52−4.63 (m, 1 H), 4.90−5.06 (m, 1 H), 6.89−7.00 (m, 2 H), 7.09−7.20 (m, 3 H), 7.45 (br s, 1 H), 7.96 (s, 1 H), 8.10 (s, 1 H), 8.20 (s, 1 H), 8.32 (br s, 1 H), 8.75 (s, 1 H). LC/MS (APCI$^+$): 460 (M + H). Anal. Calcd for $C_{25}H_{26}N_7OF{\cdot}0.75H_2O$: C, 63.63; H, 5.72; N, 20.48. Found: C, 63.48; H, 5.86; N, 20.73.

(4-Amino-7-isopropyl-7H-pyrrolo[2,3-*d*]pyrimidin-5-yl)(6-{[(1*R*,2*R*)-2-(4-fluorophenyl)cyclopentyl]methylamino}pyrazin-2-yl)methanone (19). The single enantiomer was prepared from the single enantiomer of N-Boc protected **6a** (see **18** above) as shown in Scheme 2. ^{1}H NMR (400 MHz, DMSO-d_6) δ ppm 1.39−1.48 (m, 6 H), 1.61−1.75 (m, 1 H), 1.98−2.17 (m, 5 H), 3.32 (s, 3 H), 3.50−3.59 (m, 1 H), 4.91−5.07 (m, 2 H), 6.98 (t, J = 8.8 Hz, 2 H), 7.10 (dd, J = 8.7, 5.7 Hz, 2 H), 7.49 (br s, 1 H), 8.20 (s, 1 H), 8.26 (s, 1 H), 8.27−8.31 (m, 1 H), 8.31 (s, 1 H), 8.61 (s, 1 H). LC/MS (APCI$^+$): 474 (M + H). Anal. Calcd for $C_{26}H_{28}N_7OF{\cdot}0.50H_2O$: C, 64.69; H, 5.94; N, 20.25. Found: C, 64.71; H, 6.06; N, 20.32.

(4-Amino-7-isopropyl-7H-pyrrolo[2,3-*d*]pyrimidin-5-yl){6-[(3*S*,4*R*)-4-(4-fluorophenyl)tetrahydrofuran-3-ylamino]-pyrazin-2-yl}methanone (20). Single enantiomers were obtained by separating the N-Boc derivative of **6b** using a Chiralpak AD-H column eluting with 9% methanol and 91% CO_2; the desired enantiomer eluted first and had optical rotation $[\alpha]_D^{22}$ +61 (*c* 2.28, MeOH). The Boc group was removed with HCl before coupling to **1**. ^{1}H NMR (400 MHz, DMSO-d_6) δ ppm 1.49 (d, J = 6.6 Hz, 3 H), 1.55

dx.doi.org/10.1021/jm201019k | *J. Med. Chem.* 2011, 54, 8490−8500

(d, J = 6.6 Hz, 3 H), 3.73 (q, J = 6.9 Hz, 1 H), 3.83 (dd, J = 8.7, 5.2 Hz, 1 H), 4.05 (dd, J = 8.6, 7.1 Hz, 1 H), 4.14−4.22 (m, 2 H), 4.85−4.94 (m, 1 H), 4.99 (quin, J = 6.7 Hz, 1 H), 6.96−7.04 (m, 2 H), 7.19 (dd, J = 8.7, 5.7 Hz, 1 H), 7.42 (d, J = 7.8 Hz, 1 H), 7.48 (br s, 1 H), 8.01 (s, 1 H), 8.14 (s, 1 H), 8.21 (s, 1 H), 8.29 (br s, 1 H), 8.69 (s, 1 H). LC/MS (APCI$^+$): 462 (M + H). Anal. Calcd for $C_{24}H_{24}N_7FO_2 \cdot 0.60H_2O$: C, 60.97; H, 5.30; N, 20.61. Found: C, 61.03; H, 5.38; N, 20.76.

(4-Amino-7-isopropyl-7H-pyrrolo[2,3-*d*]pyrimidin-5-yl){6-[(2*R*,3*R*)-2-(4-fluorophenyl)tetrahydrofuran-3-ylamino]-pyrazin-2-yl}methanone (21). Single enantiomers were obtained by separating the N-Boc derivative of 7 using a Chiralpak AD-H column eluting with 10% methanol and 90% CO_2 at 140 bar; the desired enantiomer eluted first and had optical rotation $[\alpha]_D^{25}$ +30 (c 0.83, MeOH). The Boc group was removed with HCl before coupling to **1**. ^{1}H NMR (300 MHz, $CDCl_3$) δ ppm 1.56 (t, 6 H), 2.11−2.27 (m, 1 H), 2.48−2.61 (m, 1 H), 4.08 (td, J = 8.5, 6.8 Hz, 1 H), 4.30 (td, J = 8.2, 5.9 Hz, 1 H), 4.48 (d, J = 7.4 Hz, 1 H), 4.73−4.87 (m, 1 H), 5.06−5.22 (m, 2 H), 7.03 (t, J = 8.7 Hz, 2 H), 7.29−7.34 (m, 2 H), 7.86 (s, 1 H), 8.35 (s, 1 H), 8.40 (s, 1 H), 8.43 (s, 1 H). LC/MS (APCI$^+$): 462 (M + H). Anal. Calcd for $C_{24}H_{24}N_7FO_2 \cdot 0.75H_2O \cdot 0.17$DMSO: C, 60.13; H, 5.33; N, 19.81. Found: C, 59.87; H, 5.47; N, 20.08.

(4-Amino-7-isopropyl-7H-pyrrolo[2,3-*d*]pyrimidin-5-yl){6-[(3*S*,4*S*)-4-(4-fluorophenyl)pyrrolidin-3-ylamino]pyrazin-2-yl}-methanone Formate Salt (22). The enantiomers were separated by chiral SFC using a Chiracel OJ-H column eluted with 30% methanol and 70% CO_2, with the desired enantiomer eluting first. The single enantiomer was repurified by preparative HPLC (acetonitrile/water gradient with formic acid). ^{1}H NMR (400 MHz, DMSO-d_6) δ ppm 1.49 (d, J = 6.8 Hz, 3 H), 1.54 (d, J = 6.6 Hz, 3 H), 3.11 (dd, J = 11.2, 3.9 Hz, 1 H), 3.23−3.35 (m, 1 H), 3.38−3.53 (m, 2 H), 3.55−3.68 (m, 1 H), 4.72−4.84 (m, 1 H), 4.98 (quin, J = 6.8 Hz, 1 H), 6.97 (t, J = 8.8 Hz, 2 H), 7.23 (dd, J = 8.3, 5.8 Hz, 2 H), 7.43 (br s, 1 H), 7.64 (d, J = 8.3 Hz, 1 H), 7.97 (s, 1 H), 8.10 (s, 1 H), 8.20 (s, 1 H), 8.29 (s, 2 H), 8.64 (s, 1 H). LC/MS (ESI$^+$): 461 (M + H). Anal. Calcd for $C_{24}H_{25}FN_8O \cdot 1.0HCO_2H \cdot 1.8H_2O$: C, 55.8; H, 5.67; N, 20.58. Found: C, 55.71; H, 5.72; N, 20.79.

(4-Amino-7-isopropyl-7H-pyrrolo[2,3-*d*]pyrimidin-5-yl){6-[(2*R*,3*R*)-2-(4-fluorophenyl)pyrrolidin-3-ylamino]pyrazin-2-yl}-methanone Formate Salt (23). The single enantiomer was synthesized from the single enantiomer of **24** (see below) as described in the text. ^{1}H NMR (400 MHz, DMSO-d_6) δ ppm 1.49 (d, J = 6.8 Hz, 3 H), 1.55 (d, J = 6.8 Hz, 3 H), 1.81−1.95 (m, 1 H), 2.19−2.31 (m, 1 H), 2.92−3.04 (m, 1 H), 3.18−3.29 (m, 1 H), 4.35 (d, J = 6.3 Hz, 1 H), 4.60−4.74 (m, 1 H), 4.99 (quin, J = 6.8 Hz, 1 H), 6.88−6.99 (m, 2 H), 7.20−7.31 (m, 3 H), 7.45 (br s, 1 H), 7.94 (s, 1 H), 8.08 (s, 1 H), 8.20 (s, 1 H), 8.30 (br s, 1 H), 8.72 (s, 1 H). LC/MS (ESI$^+$): 461 - (M + H). Anal. Calcd for $C_{24}H_{25}N_8FO \cdot 1.2HCO_2H \cdot 1.4H_2O$: C, 55.96; H, 5.54; N, 20.70. Found: C, 55.95; H, 5.63; N, 20.71.

(2*R*,3*R*)-3-[6-(4-Amino-7-isopropyl-7H-pyrrolo[2,3-*d*]-pyrimidine-5-carbonyl)pyrazin-2-ylamino]-2-(4-fluorophenyl)-pyrrolidine-1-carbaldehyde (24). The enantiomers were separated by chiral SFC using a Chiracel OD-H column eluted with 40% methanol and 60% CO_2. $[\alpha]^{22}_D$ +454 (c 0.37, MeOH). ^{1}H NMR (400 MHz, DMSO-d_6, 1.7:1 mixture of rotamers A:B) δ ppm 1.29−1.43 (m, 6 H), 1.81−2.03 (m, 1 H), 2.09−2.23 (m, 1 H), 3.29−3.40 (m, 0.6 H, rotamer A), 3.57 (td, J = 10.2, 7.1 Hz, 0.4 H, rotamer B), 3.72 (t, J = 10.5 Hz, 0.6 H, rotamer A), 3.97 (t, J = 9.3 Hz, 0.4 H, rotamer B), 4.46−4.56 (m, 0.4 H, rotamer B), 4.56−4.67 (m, 0.6 H, rotamer A), 4.87 (sxt, J = 6.8 Hz, 1 H), 5.13 (d, J = 7.3 Hz, 0.4 H, rotamer B), 5.26 (d, J = 7.3 Hz, 0.6 H, rotamer A), 6.83−6.92 (m, 2 H), 6.92−6.99 (m, 0.7 H, rotamer B), 6.99−7.06 (m, 1.3 H, rotamer A), 7.27 (d, J = 6.8 Hz, 0.4 H, rotamer B), 7.32 (d, J = 6.8 Hz, 0.6 H, rotamer A), 7.39 (br s, 1 H), 7.92 (s, 0.4 H, rotamer B), 7.94 (s, 0.6 H, rotamer A), 8.02 (s, 0.6 H, rotamer A), 8.12 (s, 1 H), 8.16 (s, 0.4 H, rotamer B), 8.22 (s, 0.4 H, rotamer B), 8.23 (s, 0.6 H, rotamer A), 8.26 (br s, 1 H), 8.77 (s, 0.4 H, rotamer B), 8.82 (s, 0.6 H, rotamer A). LC/MS (APCI$^+$): 489 (M + H). Anal. Calcd for $C_{25}H_{25}N_8FO_2 \cdot 1.80H_2O$: C, 57.58; H, 5.4; N, 21.59. Found: C, 57.64; H, 5.53; N, 21.51.

1-[(2*R*,3*R*)-3-[6-(4-Amino-7-isopropyl-7H-pyrrolo[2,3-*d*]-pyrimidine-5-carbonyl)pyrazin-2-ylamino]-2-(4-fluorophenyl)-pyrrolidin-1-yl]ethanone (25). The enantiomers were separated by chiral SFC using a Chiracel OD-H column eluted with 40% methanol and 60% CO_2. $[\alpha]^{22}_D$ +595 (c 0.21, MeOH). ^{1}H NMR (400 MHz, DMSO-d_6, 1.4:1 mixture of rotamers A:B) δ ppm 1.37−1.50 (m, 6 H), 1.59 (s, 1.3 H, rotamer B), 2.00 (s, 1.7 H, rotamer A), 1.93−2.09 (m, 1 H), 2.16−2.30 (m, 1 H), 3.37−3.45 (m, 0.4 H, rotamer B), 3.52−3.64 (m, 0.6 H, rotamer A), 3.83 (t, J = 10.5 Hz, 0.4 H, rotamer B), 3.98 (t, J = 9.5 Hz, 0.6 H, rotamer A), 4.48−4.61 (m, 0.6 H, rotamer A), 4.70−4.84 (m, 0.4 H, rotamer B), 4.88−5.04 (m, 1 H), 5.21 (d, J = 7.3 Hz, 0.4 H, rotamer B), 5.26 (d, J = 7.3 Hz, 0.6 H, rotamer A), 6.87−6.96 (m, 1.2 H, rotamer A), 6.96−7.09 (m, 2 H), 7.14 (t, J = 8.7 Hz, 0.8 H, rotamer B), 7.26 (d, J = 6.8 Hz, 0.4 H, rotamer B), 7.35 (d, J = 6.6 Hz, 0.6 H, rotamer A), 7.48 (br s, 1 H), 8.02 (s, 1 H), 8.20 (s, 1 H), 8.33 (s, 1 H), 8.34 (br s, 1 H), 8.92 (s, 1 H). LC/MS (APCI$^+$): 503 (M + H). Anal. Calcd for $C_{26}H_{27}N_8FO_2 \cdot 0.70H_2O$: C, 60.71; H, 5.48; N, 21.61. Found: C, 60.62; H, 5.56; N, 21.75.

1-{(2*R*,3*R*)-3-[6-(4-Amino-7-isopropyl-7H-pyrrolo[2,3-*d*]-pyrimidine-5-carbonyl)pyrazin-2-ylamino]-2-phenylpyrrolidin-1-yl}ethanone (26). The single enantiomer was obtained by separating intermediate **13a** using a Chiralpak AS-H column eluted with 20% methanol and 80% CO_2; the desired enantiomer of **13a** was the (+) isomer. ^{1}H NMR (400 MHz, DMSO-d_6, 1.3:1 mixture of rotamers A:B) δ ppm 1.36−1.50 (m, 6 H), 1.56 (s, 1.3 H, rotamer B), 2.00 (s, 1.7 H, rotamer A), 2.02−2.14 (m, 1 H), 2.16−2.31 (m, 1 H), 3.37−3.47 (m, 0.4 H, rotamer B), 3.60 (td, J = 10.7, 6.3 Hz, 0.6 H, rotamer A), 3.77−3.88 (m, 0.4 H, rotamer B), 3.98 (t, J = 9.1 Hz, 0.6 H, rotamer A), 4.47−4.62 (m, 0.6 H, rotamer A), 4.71−4.83 (m, 0.4 H, rotamer B), 4.91−5.01 (m, 1 H), 5.20 (d, J = 7.3 Hz, 0.4 H, rotamer B), 5.29 (d, J = 7.3 Hz, 0.6 H, rotamer A), 6.89 (d, J = 7.1 Hz, 1.1 H, rotamer A), 6.94 (d, J = 7.1 Hz, 0.9 H, rotamer B), 7.13−7.25 (m, 1.7 H, rotamer A), 7.25−7.34 (m, 1.3 H, rotamer B plus 0.4 H, rotamer B), 7.37 (d, J = 7.1 Hz, 0.6 H, rotamer A), 7.48 (br s, 1 H), 8.00 (s, 1 H), 8.20 (s, 1 H), 8.32 (s, 0.4 H, rotamer B), 8.33 (s, 0.6 H, rotamer A), 8.36 (br s, 1 H), 8.94 (s, 1 H). LC/MS (ESI$^+$): 485 (M + H). Anal. Calcd for $C_{26}H_{28}N_8O_2 \cdot 2.0H_2O$: C, 60.21; H, 5.98; N, 21.29. Found: C, 59.99; H, 6.20; N, 21.52.

■ ASSOCIATED CONTENT

Ⓢ Supporting Information

Further experimental details; full kinase profiling from Invitrogen for analogues **24**, **25**, and **26**; and crystallographic methods and data for **15** and **20** in PDK1. This material is available free of charge via the Internet at http://pubs.acs.org.

Accession Codes

PDB nos.: cmpd **15** in PDK1, 3RWQ; cmpd **20** in PDK1, 3RWP.

■ AUTHOR INFORMATION

Corresponding Author

*Present address: Takeda San Diego, 10410 Science Center Drive, San Diego, CA 92121. E-mail: sean.murphy@takedasd.com. Phone: 858-731-3596.

■ ACKNOWLEDGMENTS

We thank Deepak Dalvie for biotransformation analysis; Muhammad Alimuddin, Christine Aurigemma, Jason Ewanicki, and Jeff Ellerass for analytical support; and Paul Richardson and Kevin Bunker for synthetic support.

■ ABBREVIATIONS USED

ADME, absorption, distribution, metabolism, and excretion; APCI, atmospheric pressure chemical ionization; ATP, adenosine triphosphate; CHAPS, 3-[(3-cholamidopropyl)-dimethylammonio]-1-propanesulfonate; CYP, cytochrome P450; 4-DMAP, *N*,*N*-dimethyl-4-aminopyridine; DTT, dithiothreitol; EDTA, ethylenediaminetetraacetic acid; EGTA, ethylene glycol tetraacetic acid; ESI, electrospray ionization; GST,

glutathione S-transferase; Hepes, 4-(2-hydroxyethyl)-1-piperazineethanesulfonic acid; HLM, human liver microsome; LE, ligand efficiency; PDK1, 3-phosphoinositide-dependent kinase; PH, pleckstrin homology; PI3K, phosphoinositide-3 kinase; PIP_3, phosphaditylinositol-(3,4,5)-triphosphate; PTEN, phosphatase and tensin homologue; SFC, supercritical fluid chromatography; RTK, receptor tyrosine kinase; TAMRA, tetramethylrhodamine; T308, threonine-308; TR-FRET, time-resolved fluorescence resonance energy transfer; Tris, tris-(hydroxymethyl) aminomethane; Ts, 4-toluenesulfonyl

REFERENCES

(1) Kobayashi, T.; Cohen, P. Activation of serum- and glucocorticoid-regulated protein kinase by agonists that activate phosphatidylinositide 3-kinase is mediated by 3-phosphoinositide-dependent protein kinase-1 (PDK1) and PDK2. *Biochem. J.* **1999**, *339*, 319−328.

(2) Mora, A.; Komander, D.; van Aalten, D. M.; Alessi, D. R. PDK1, the master regulator of AGC kinase signal transduction. *Semin. Cell Dev. Biol.* **2004**, *Apr 15*, 161−170.

(3) Raimondi, C.; Falasca, M. Targeting PDK1 in Cancer. *Curr. Med. Chem.* **2011**, *18*, 2763−2769.

(4) Bayascas, J. R.; Leslie, N. R.; Parsons, R.; Fleming, S.; Alessi, D. R. Hypomorphic mutation of PDK1 suppresses tumorigenesis in PTEN(±) mice. *Curr. Biol.* **2005**, *15*, 1839−1846.

(5) Zeng, X.; Xu, H.; Glazer, R. I. Transformation of mammary epithelial cells by 3-phosphoinositide-dependent protein kinase-1 (PDK1) is associated with the induction of protein kinase Calpha. *Cancer Res.* **2002**, *62*, 3538−3543.

(6) Li, Y.; Yang, K. J.; Park, J. Multiple implications of 3-phosphoinositide-dependent protein kinase 1 in human cancer. *World J. Biol. Chem.* **2010**, *1*, 239−247.

(7) Peifer, C.; Alessi, D. R. Small-molecule inhibitors of PDK1. *ChemMedChem* **2008**, *3*, 1810−1838.

(8) Angiolini, M.; Banfi, P.; Casale, E.; Casuscelli, F.; Fiorelli, C.; Saccardo, M. B.; Silvagni, M.; Zuccotto, F. Structure-based optimization of potent PDK1 inhibitors. *Bioorg. Med. Chem. Lett.* **2010**, *20*, 4095−4099.

(9) Najafov, A.; Sommer, E. M.; Axten, J. M.; Deyoung, M. P.; Alessi, D. R. Characterization of GSK2334470, a novel and highly specific inhibitor of PDK1. *Biochem. J.* **2010**, *433*, 357−369.

(10) Nagashima, K.; Shumway, S. D.; Sathyanarayanan, S.; Chen, A. H.; Dolinski, B.; Xu, Y.; Keilhack, H.; Nguyen, T.; Wiznerowicz, M.; Li, L.; Lutterbach, B. A.; Chi, A.; Paweletz, C.; Allison, T.; Yan, Y.; Munshi, S. K.; Klippel, A.; Kraus, M.; Bobkova, E. V.; Deshmukh, S.; Xu, Z.; Mueller, U.; Szewczak, A. A.; Pan, B. S.; Richon, V.; Pollock, R.; Blume-Jensen, P.; Northrup, A.; Andersen, J. N. Genetic and pharmacological inhibition of PDK1 in cancer cells: Characterization of a selective allosteric kinase inhibitor. *J. Biol. Chem.* **2011**, *286*, 6433−6448.

(11) (a) Islam, I.; Bryant, J.; Chou, Y. L.; Kochanny, M. J.; Lee, W.; Phillips, G. B.; Yu, H.; Adler, M.; Whitlow, M.; Ho, E.; Lentz, D.; Polokoff, M. A.; Subramanyam, B.; Wu, J. M.; Zhu, D.; Feldman, R. I.; Arnaiz, D. O. Indolinone based phosphoinositide-dependent kinase-1 (PDK1) inhibitors. Part 1: Design, synthesis and biological activity. *Bioorg. Med. Chem. Lett.* **2007**, *17*, 3814−3818. (b) Islam, I.; Brown, G.; Bryant, J.; Hrvatin, P.; Kochanny, M. J.; Phillips, G. B.; Yuan, S.; Adler, M.; Whitlow, M.; Lentz, D.; Polokoff, M. A.; Wu, J.; Shen, J.; Walters, J.; Ho, E.; Subramanyam, B.; Zhu, D.; Feldman, R. I.; Arnaiz, D. O. Indolinone based phosphoinositide-dependent kinase-1 (PDK1) inhibitors. Part 2: Optimization of BX-517. *Bioorg. Med. Chem. Lett.* **2007**, *17*, 3819−3825.

(12) Gopalsamy, A.; Shi, M.; Boschelli, D. H.; Williamson, R.; Olland, A.; Hu, Y.; Krishnamurthy, G.; Han, X.; Arndt, K.; Guo, B. Discovery of dibenzo[c,f][2,7]naphthyridines as potent and selective 3-phosphoinositide-dependent kinase-1 inhibitors. *J. Med. Chem.* **2007**, *50*, 5547−5549.

(13) Stauffer, F.; Maira, S. M.; Furet, P.; García-Echeverría, C. Imidazo[4,5-c]quinolines as inhibitors of the PI3K/PKB-pathway. *Bioorg. Med. Chem. Lett.* **2008**, *18*, 1027−1030.

(14) Karaman, M. W.; Herrgard, S.; Treiber, D. K.; Gallant, P.; Atteridge, C. E.; Campbell, B. T.; Chan, K. W.; Ciceri, P.; Davis, M. I.; Edeen, P. T.; Faraoni, R.; Floyd, M.; Hunt, J. P.; Lockhart, D. J.; Milanov, Z. V.; Morrison, M. J.; Pallares, G.; Patel, H. K.; Pritchard, S.; Wodicka, L. M.; Zarrinkar, P. P. A quantitative analysis of kinase inhibitor selectivity. *Nat. Biotechnol.* **2008**, *26*, 127−132.

(15) Lind, K. E.; Lin, E. Y.; Nguyen, T. B.; Tangonan, B. T.; Cao, K.; Erlanson, D. A.; Guckian, K.; Simmons, R. L.; Lee, W.; Sun, L.; Hansen, S.; Pathan, N.; Zhang, L. Pyridinonyl PDK1 inhibitors. *PCT Int. Appl.* 2008, WO2008/5457 A2.

(16) Shepherd, T. A.; Aikins, J. A.; Bleakman, D.; Cantrell, B. E.; Rearick, J. P.; Simon, R. L.; Smith, E. C. R.; Stephenson, G. A.; Zimmerman, D. M.; Mandelzys, A.; Jarvie, K. R.; Ho, K.; Deverill, M.; Kamboj, R. K. Design and synthesis of a novel series of 1,2-disubstituted cyclopentanes as small, potent potentiators of 2-amino-3-(3-hydroxy-5-methyl-isoxazol-4-yl)propanoic acid (AMPA) receptors. *J. Med. Chem.* **2002**, *45*, 2101−2111.

(17) Andreotti, D.; Ward, S. E. Preparation of N-[2-phenyl-tetrahydrofuran-3-yl]-2-propanesulfonamide derivatives as glutamate receptor modulators. *PCT Int. Appl.* 2007, WO2007090841.

(18) Xu, Z.; Lu, X. Phosphine-catalyzed [3 + 2] cycloaddition reactions of substituted 2-alkynoates or 2,3-allenoates with electron-deficient olefins and imines. *Tetrahedron Lett.* **1999**, *40* (3), 549−552.

(19) Hopkins, A. L.; Groom, C. R.; Alex, A. Ligand efficiency: A useful metric for lead selection. *Drug Discovery Today* **2004**, *9*, 430−431.

(20) Michel, J.; Tirado-Rives, J.; Jorgensen, W. L. Energetics of displacing water molecules from protein binding sites: Consequences for ligand optimization. *J. Am. Chem. Soc.* **2009**, *131*, 15403−15411.

(21) Zlokarnik, G.; Grootenhuis, P. D. J.; Watson, J. B. High throughput P450 inhibition screens in early drug discovery. *Drug Discovery Today* **2005**, *10*, 1443−1450.

(22) PI3K-γ crystal structures were used as a surrogate for developing binding hypotheses for PI3K-α, which was used in the enzymatic assay. The crystal structure of **16** in PI3K-γ is available from the PDB, entry 2V4L.

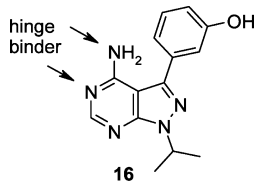

16

(23) Andrews, P. R.; Craik, D. J.; Martin, J. L. Functional group contributions to drug−receptor interactions. *J. Med. Chem.* **1984**, *27*, 1648−1657.

(24) Gleeson, M. P. Generation of a set of simple, interpretable ADMET rules of thumb. *J. Med. Chem.* **2008**, *51*, 817−834.

(25) Analiza Inc., 3615 Superior Avenue, Suite 4407B, Cleveland, OH 44114. Solubility assay: http://www.analiza.com/adme/aqueous-solubility.html.

(26) The LE from **14** to **24** decreased from 0.42 to 0.38. A decrease in LE is often observed during lead optimization. Researchers at Johnson and Johnson (Reynolds, C. H.; Tounge, B. A.; Bembenek, S. D. Ligand binding efficiency: Trends, physical basis, and implications. *J. Med. Chem.* **2008**, *51*, 2432−2438,) have suggested causes for this effect and introduced the Fit Quality parameter to account for it. The Fit Quality from **14** to **24** increases from 0.73 to 0.89 and indicates an efficient use of heavy atoms in the optimization process.

(27) Liu, K.; Zhu, J.; Smith, G. L.; Yin, M.; Bailey, S.; Chen, J. H.; Hu, Q.; Huang, Q.; Li, C.; Li, Q. J.; Marx, M. A.; Paderes, G.; Richardson, P. F.; Sach, N. W.; Walls, M.; Wells, P. A.; Zou, A. Highly selective and potent thiophenes as PI3K inhibitors with oral antitumor activity. *Med. Chem. Lett.* **2011**, *2*, 809−813.

(28) Johnson, T. W.; Bailey, S.; Baxi, S. M.; Brooun, A.; Dinh, D. M.; He, M.; Hoffman, J. E.; Kan, J. L. C.; Lam, H.; Li, C.; Mehta, P. P.; Sach, N. W.; Smeal, T.; Walls, M.; Wells, P.; Yin, M.; Yu, X.; Zou, A. The chemistry and biology of mTOR selective inhibitors. *AACR Special Conference: Targeting PI3K/mTOR Signaling in Cancer*, Feb. 24−27, 2011, San Francisco, CA.

(29) Hofler, A.; Nichols, T.; Grant, S.; Lingardo, L.; Esposito, E. A.; Gridley, S.; Murphy, S. T.; Kath, J. C.; Cronin, C. N.; Kraus, M.; Alton, G.; Xie, Z.; Sutton, S.; Gehring, M.; Ermolieff, J. Study of the PDK1/AKT signaling pathway using selective PDK1 inhibitors, HCS, and enhanced biochemical assays. *Anal. Biochem.* **2011**, *414*, 179−186.

(30) *GraphPad Prism*, version 5.01; GraphPad Software Inc.: San Diego.

(31) Morrison, J. F. Kinetics of the reversible inhibition of enzyme catalysed reactions by tight-binding inhibitors. *Biochim. Biophys. Acta* **1969**, *185*, 269−286.